AAC Journals.ASM.org

In Vitro and *In Vivo* Evaluation of 28DAP010, a Novel Diamidine for Treatment of Second-Stage African Sleeping Sickness

Tanja Wenzler,[a,b] Sihyung Yang,[c] Donald A. Patrick,[d] Olivier Braissant,[b,e] Mohamed A. Ismail,[f] Richard R. Tidwell,[d] David W. Boykin,[f] Michael Zhuo Wang,[c] Reto Brun[a,b]

Medical Parasitology & Infection Biology, Swiss Tropical and Public Health Institute, Basel, Switzerland[a]; University of Basel, Basel, Switzerland[b]; Department of Pharmaceutical Chemistry, School of Pharmacy, The University of Kansas, Lawrence, Kansas, USA[c]; Department of Pathology and Laboratory Medicine, School of Medicine, University of North Carolina, Chapel Hill, North Carolina, USA[d]; Department of Urology, University Hospital of Basel, Basel, Switzerland[e]; Department of Chemistry, Georgia State University, Atlanta, Georgia, USA[f]

African sleeping sickness is a neglected tropical disease transmitted by tsetse flies. New and better drugs are still needed especially for its second stage, which is fatal if untreated. 28DAP010, a dipyridylbenzene analogue of DB829, is the second simple diamidine found to cure mice with central nervous system infections by a parenteral route of administration. 28DAP010 showed efficacy similar to that of DB829 in dose-response studies in mouse models of first- and second-stage African sleeping sickness. The *in vitro* time to kill, determined by microcalorimetry, and the parasite clearance time in mice were shorter for 28DAP010 than for DB829. No cross-resistance was observed between 28DAP010 and pentamidine on the tested *Trypanosoma brucei gambiense* isolates from melarsoprol-refractory patients. 28DAP010 is the second promising preclinical candidate among the diamidines for the treatment of second-stage African sleeping sickness.

African sleeping sickness, also known as human African trypanosomiasis (HAT), is a tropical disease that threatens millions of people living in sub-Saharan Africa (1). It is caused by two subspecies of the single-celled parasite *Trypanosoma brucei*, *Trypanosoma brucei gambiense* and *Trypanosoma brucei rhodesiense*. The protozoans are transmitted by the bite of infected tsetse flies. The disease is fatal without effective treatment. The burden of the disease has been reduced to some extent by increased control interventions, but the disease is still one of the most neglected tropical diseases, and it is estimated by the WHO that there are still 25,000 to 30,000 infected patients (2, 3).

HAT progresses in two stages. In the first stage, the parasites reside in the blood and the lymphatic system. In the second stage, the parasites cross the blood-brain barrier (BBB) and spread the infection to the central nervous system (CNS), leading to neurological and psychiatric disorders, including irregular and fragmented sleeping patterns, behavioral changes, motor weakness, coma, and ultimately death (4).

Patients can be cured only by effective and safe drugs. Vaccines are not available and are unlikely to be developed in the near future, and self-healing through the body's own immune system is also not possible due to antigenic variation of the surface glycoproteins of the parasites (5). The drugs currently available have serious disadvantages such as adverse effects, limited efficacy, complicated treatment schedules, and the need for parenteral administration. New drugs are therefore needed, especially for the second stage of the disease.

In the search for new drugs, aromatic diamidines are seen as promising candidates for use against HAT. These compounds are known to have a broad spectrum of antiprotozoal activities (6). Pentamidine has been in use since the 1940s for first-stage *T. b. gambiense* HAT and against leishmaniasis and *Pneumocystis jirovecii* pneumonia (7). Diminazene (8) and isometamidium (a monoamidine) are used to treat animal trypanosomiasis. Therefore, considerable effort has been put into the synthesis and investigation of novel aromatic diamidines with improved properties for use against HAT.

One problem with diamidines is that they are protonated at physiological pH and therefore do not easily cross the gastrointestinal tract and the BBB by diffusion. Their cationic nature was therefore believed to reduce their potential for use as oral drugs and to reduce their efficacy against second-stage HAT by any route of administration; therefore, much effort went into the design of prodrugs (6, 9). Prodrugs are inactive against trypanosomes *in vitro* but can be metabolized to the active diamidine molecules by host enzymes upon administration *in vivo* (10–12), thus serving as potentially orally active drugs. The prodrug approach worked well with regard to oral bioavailability in animal models (9, 13, 14) as well as in humans, in whom the prodrug DB289 (pafuramidine maleate) underwent clinical trials as the first oral drug for treatment of first-stage HAT patients (15, 16). Several other prodrugs have been tested in the second-stage mouse model, but few of them were able to cure CNS infections in mice (14, 17).

During a series of tests in our laboratory, we discovered that the diamidine DB829 was intrinsically active in second-stage animal models (14, 18). This was unexpected, as simple diamidines (amidines without substituents on either nitrogen atom) are thought to be unable to cross the BBB by diffusion due to their cationic

Received 25 October 2013 **Returned for modification** 12 January 2014
Accepted 14 May 2014
Published ahead of print 27 May 2014
Address correspondence to Tanja Wenzler, Tanja.Wenzler@unibas.ch.
Supplemental material for this article may be found at http://dx.doi.org/10.1128/AAC.02309-13.

doi:10.1128/AAC.02309-13

nature. For many years, DB829 remained the only diamidine that showed high CNS activity *in vivo* (14, 19).

Recently, we found that 28DAP010 (also known as CPD0905) and its close analogues 19DAP025 and 27DAP060 were highly active *in vitro* against *T. b. rhodesiense* and were curative in the stringent *T. b. rhodesiense* STIB900 first-stage mouse model at the low dose of 4 × 5 mg/kg of body weight (i.e., daily dose of 5 mg/kg given on 4 consecutive days) or as a single dose of 10 mg/kg by an intraperitoneal (i.p.) route of administration (20). In this paper, we present more data from our investigations of this new novel diamidine with high CNS activity *in vivo*, 28DAP010, and its analogues 19DAP025 and 27DAP060. We performed a full dose-response experiment in the STIB900 acute-stage mouse model to determine the minimal curative dose for the three compounds and evaluated their CNS activity in the GVR35 CNS mouse model. As 28DAP010 showed better efficacy than the analogues, we carried out a detailed biological characterization of this compound. We collected *in vitro* data on different *T. brucei* strains and subspecies, with a particular emphasis on trypanocidal activity on *T. b. gambiense*, as the majority (>98%) of African sleeping sickness patients are infected with *T. b. gambiense* (2). Additionally, we assessed the time to kill of 28DAP010 *in vitro* using microcalorimetry, a new method to measure drug activity on a real-time basis (21). This was important, because aromatic diamidines typically kill the trypanosomes rather slowly, with a time to kill of about 24 to 48 h after treatment (22). Among the diamidines, DB829 was one of the slowest-acting compounds, with a time to kill of >48 h (23). After having analyzed the pharmacokinetic properties of 28DAP010 in mice at a curative single dose, we assessed the parasite clearance time at an identical dose in mice infected with *T. b. rhodesiense* and *T. b. gambiense* strains.

MATERIALS AND METHODS

Materials. Pentamidine isethionate was purchased from Sigma-Aldrich (St. Louis, MO). Syntheses of 28DAP010 (CPD-0905) (20), 19DAP025 (20), 27DAP060 (20), DB829 (24), DB1244 (20) and deuterium-labeled DB75 (DB75-d8; deuterated phenyl rings; internal standard) (25), all isolated as their hydrochloride salts, have been previously reported.

Antitrypanosomal activities of 28DAP010 and pentamidine *in vitro*.
(i) Preparation of compounds. Compounds were dissolved in 100% dimethyl sulfoxide (DMSO) and finally diluted in culture medium prior to the *in vitro* assay. The DMSO concentration never exceeded 1% in the *in vitro* alamarBlue assays at the highest drug concentration. For microcalorimetry assays, the DMSO concentration was kept at 0.1% in all samples.

(ii) Parasites. The *T. brucei* strains used in this study are described in Table 1.

(iii) *In vitro* growth inhibition assays using *T. brucei* subspecies. The 50% inhibitory concentrations (IC_{50}s) were determined using the alamarBlue assay as described by Räz et al. (26), with a 3-day drug exposure and minor modifications as described previously (23). Assays were carried out at least three times independently and each time in duplicate. The IC_{50}s are the means of the independent assays. Coefficients of variation were less than 50%. Different culture and assay media were used for *T. b. gambiense* and *T. b. rhodesiense*, as previously described by Wenzler et al. (23).

(iv) Microcalorimetry studies using *T. brucei* subspecies. *In vitro* time of drug action was monitored using isothermal microcalorimetry. With this method, the time of drug action on a parasite population can be determined on a real-time basis (21, 23). The strain STIB900 was used as a representative for *T. b. rhodesiense* and STIB930 (and sometimes additionally ITMAP141267) for *T. b. gambiense*.

For experiments with continuous drug exposure, bloodstream trypanosomes (2 ml at 5×10^4/ml per ampoule) were spiked with different concentrations of 28DAP010, with a final DMSO concentration of 0.1% (vol/vol). Negative controls contained culture medium only. The heat flow was continuously measured (1 reading/second) at 37°C in the isothermal microcalorimetry instrument (thermal activity monitor, model 249 TAM III). Each experiment with continuous drug exposure was set up in triplicate and carried out a total of 3 times (21).

(v) Inoculum studies. For studies of the drug effect on different parasite densities in the inoculum, the parasite density was reduced to 1×10^4/ml of bloodstream trypanosomes and supplemented with 28DAP010 at the desired concentrations. Inhibition of growth and viability was compared with that in the samples containing the standard inoculum of 5×10^4/ml of bloodstream trypanosomes and the same drug concentrations (23). Each experiment was set up in triplicate and repeated once.

(vi) Drug wash-out experiments. For the 24-h exposure experiment, trypanosomes (*T. b. rhodesiense* strain STIB900 and *T. b. gambiense* strain STIB930) were incubated with 28DAP010 for 24 h at 37°C and then washed twice to remove the compound. Subsequently, the washed trypanosomes were resuspended in drug-free culture medium, transferred to ampoules, and inserted into the isothermal microcalorimetry instrument. The drug-free control samples (drug free, wash-out) were washed identically to the drug-containing samples. Each 24-h exposure experiment was set up in triplicate and repeated once (23).

(vii) Analysis of microcalorimetry heat flow data. To facilitate further calculations, the recorded data were resampled to obtain an effective sampling frequency of 1 data point per 1.5 min, using the manufacturer's software (TAM assistant version v1.2.4.0), and exported to a spreadsheet. Forty-five minutes was added to the time data to account for the preparation of the ampoules and the transfer from the bench to the calorimeter. Resulting data were plotted as heat flow (in μW) over time. Each single curve for heat flow (in watts) over time was analyzed using the R statistical package (27). Data were smoothed using a cubic spline (smooth.spline function) in the R statistical software (27–30). The time to onset of drug action was determined as the time at which a divergence between the heat flow of the drug-free controls and the drug-containing specimens could be observed. The time to peak was determined as the time point at which the highest heat flow was measured for each samples. The time to kill the parasite population was defined as the time point when the heat production was reduced to the level of the sterile medium control (base level) (23).The growth rate (μ) of each culture was calculated using the heat-over-time data (integrated heat flow data over time). For this calculation, the Gompertz growth model was fitted over the whole curve using R software and the Grofit package as described previously (23, 31). The growth rate calculated based on the heat released by the metabolic activity

TABLE 1 *T. brucei* isolates used in this study

Trypanosome strain(s)[a]	Subspecies	Year of isolation	Origin	Reference
STIB900, STIB704	*T. b. rhodesiense*	1982	Tanzania	52
BS221, S427	*T. b. brucei*	1960	Uganda	42
BS221Δ*AT1*	*T. b. brucei*			42
GVR35, S10	*T. b. brucei*	1966	Serengeti	53
STIB930, STIB754	*T. b. gambiense*	1978	Côte d'Ivoire	54
ITMAP141267	*T. b. gambiense*	1960	DRC	55
130R	*T. b. gambiense*	2005	DRC	56
40R	*T. b. gambiense*	2005	DRC	56
45R	*T. b. gambiense*	2005	DRC	56
349R	*T. b. gambiense*	2006	DRC	56
DAL898R	*T. b. gambiense*	1985	Côte d'Ivoire	52
K03048	*T. b. gambiense*	2003	South Sudan	57

[a] Strains labeled with an "R" were isolated from patients after a relapse after melarsoprol treatment.

in the culture is considered only as a proxy for the growth rate calculated from the exponential growth phase by conventional approaches, since lysis and chemical processes due to the nature of the medium might also contribute to the overall heat signal (23, 31).

***In vivo* studies. (i) Efficacy and time to kill in mice.** The efficacy and time-to-kill experiments were performed at the Swiss Tropical and Public Health Institute. Adult female NMRI (Naval Medical Research Institute) mice were obtained from Janvier, France, or from Harlan, the Netherlands. They weighed between 20 and 25 g at the beginning of the study and were housed under standard conditions with food pellets and water *ad libitum*. All protocols and procedures were reviewed and approved by the veterinary authorities of Canton Basel-Stadt, Switzerland. For experiments with mice, the compounds were dissolved in DMSO and further diluted with distilled water to a final DMSO concentration of 10% prior to administration to the animals.

(ii) Efficacy in an acute-stage *T. b. rhodesiense* STIB900 mouse model. The STIB900 acute-stage mouse model mimics the first (hemolymphatic) stage of HAT. Experiments were performed as previously reported (23). Briefly, four female NMRI mice per group were infected intraperitoneally (i.p.) with 5×10^3 STIB900 bloodstream forms. Drug administration (i.p.) began 3 days after infection. A control group was infected but remained untreated. All mice were monitored for parasitemia by microscopic examination of tail blood twice a week until day 30, followed by once a week until 60 days after infection. The time to parasite relapse was recorded to calculate the mean relapse time in days after infection. Mice were euthanized after parasitemia relapse detection. Mice were considered cured if they survived and were aparasitemic until day 60.

(iii) Efficacy in acute-stage *T. b. gambiense* mouse models. Experiments were performed as previously reported (23). Briefly, four female NMRI mice per group were immunosuppressed with 200 mg/kg of cyclophosphamide (Endoxan, Baxter, Deerfield, IL) 2 days prior to infection with 10^5 bloodstream forms with one of the four *T. b. gambiense* strains (i.e., ITMAP141267, STIB930, 130R, or 45R). Immunosuppression with cyclophosphamide followed every second week until the end of the experiment. Drug administration (i.p.) began 3 days after infection. A control group was infected but remained untreated. Mice were monitored for parasitemia twice a week until day 30 and then once a week until 90 days after infection. Mice were considered cured if they survived and were aparasitemic until day 90.

(iv) Efficacy in a CNS stage *T. b. brucei* GVR35 mouse model. The GVR35 mouse CNS model mimics the second stage of the disease. GVR35 is a less virulent strain than STIB900 and crosses the BBB of mice around 7 days after infection (32). Experiments were performed as previously reported (14), with minor modifications. Five female NMRI mice per experimental group were used. Each mouse was inoculated i.p. with 2×10^4 bloodstream forms. The drug administration was i.p. for diamidines and *per os* (p.o.) for prodrugs on five consecutive days from day 17 to 21 after infection. Some experimental groups were treated for 10 consecutive days (day 17 to 26 after infection). A negative-control group was treated on day 17 with a single dose of diminazene aceturate at 40 mg/kg of body weight i.p., which is subcurative since it clears the trypanosomes only from the hemolymphatic system and not from the CNS, leading to a subsequent reappearance of trypanosomes in the blood (33). Parasitemia was monitored twice a week from the time after treatment until day 50 after infection, followed by once a week until 180 days after infection. Mice were considered cured when there was no parasitemia relapse detected over the 180-day observation period. Surviving and aparasitemic mice were euthanized on day 180.

(v) *In vivo* time to kill. Infection with *T. b. rhodesiense* and *T. b. gambiense* and immunosuppression for *T. b. gambiense*-infected mice were carried out as described for the efficacy experiments. In different mouse models the parasite load varied, an observation that was also made in the efficacy experiments. Mice were treated with a single dose of 20 mg/kg i.p. 3 days postinfection. The first microscopic examination of blood was done 24 h after treatment, and examination was done subsequently twice per day until all parasites had disappeared. When microscopy was not sensitive enough to detect any parasites, a hematocrit buffy coat examination was performed. The first time point at which no trypanosomes were detected on the microscopic slide or in the buffy coat was considered the clearance time (or time to kill) in mice. The detection limit by buffy coat examination was <100 trypanosomes/ml of blood. Mice were kept and further observed by tail blood examination until the end of the experiment to verify whether the administered dose was curative in the infected mice (23).

Pharmacokinetic studies. (i) Animals for PK studies. The pharmacokinetic (PK) studies were performed at the University of Kansas. Protocols for the animal studies were approved by the Institutional Animal Care and Use Committee of the University of Kansas. Male Swiss Webster mice (weighing 20 to 25 g) were purchased from the Charles River Laboratories (O'Fallon, MO). Mice were housed in a clean room under filtered, pathogen-free air, in a 12-h light/dark cycle, and with food pellets and water available *ad libitum*. Although a different strain and sex of mice were used in our PK studies compared to efficacy studies, we did not expect that diamidine PK would differ significantly between different strain and sex of mice.

(ii) Pharmacokinetics and brain exposure in mice. The single-dose pharmacokinetics of 28DAP010 was evaluated in mice (in triplicate) after intravenous (i.v.) and i.p. administration. 28DAP010 was dissolved in sterile saline. The doses were 7.5 μmol/kg (approximately 2.4 mg/kg) for i.v. administration and 65 μmol/kg (approximately 21 mg/kg) for i.p. administration, which was the dose used in the *in vivo* time-to-kill study. The dose volume was 5 ml/kg. No overt adverse effects were observed in mice at these dose levels. Blood sampling occurred at 0.25, 0.5, 1, 2, 4, 6, 8, 12, 24, 48, and 72 h postdose. Additional earlier sampling times, at 0.0167 and 0.083 h, were included for the i.v. administration. Blood was collected via the submandibular vein (~0.04 ml per bleed) or heart (~0.8 ml) into lithium heparin-coated Microvette tubes (Sarstedt Inc., Newton, NC). Terminal blood and brain samples were collected at 4, 12, and 72 h postdose. Plasma was obtained by centrifugation. Excised mouse brain samples were quickly rinsed with distilled water, blotted dry with tissue paper, and weighed. All samples were stored at −20°C until further processing for quantification by ultrahigh-performance liquid chromatography-tandem mass spectrometry (UPLC-MS/MS).

(iii) Plasma and tissue binding assays. Binding of 28DAP010 to mouse plasma and brain was evaluated by the equilibrium dialysis method using a rapid equilibrium dialysis device (Thermo Scientific Pierce, Rockford, IL) as previously described (34). Briefly, blank (untreated and uninfected) mouse brains were collected and homogenized in 2 volumes (vol/wt) of water (3-fold dilution). 28DAP010 was spiked into blank plasma or brain homogenates to yield a final drug concentration of 1 μM. Spiked plasma or brain homogenates (in triplicate) were added to the dialysis device and dialyzed against phosphate-buffered saline (PBS) for 6 h at 37°C to reach equilibrium between the plasma/tissue compartment and the buffer compartment. At the end of incubation, samples from the plasma/tissue compartment and the buffer compartment were collected and analyzed for total and unbound concentrations by UPLC-MS/MS. Unbound fractions in the mouse brain ($f_{u,\,brain}$) were calculated by correcting for dilution (35).

(iv) UPLC-MS/MS analysis. (*a*) Sample preparation. Plasma samples (2 μl) were mixed with 200 μl of 7:1 (vol/vol) methanol-water containing 0.1% trifluoroacetic acid and an internal standard (1 nM DB75-d8) and then vortex mixed for 30 s, followed by centrifugation (2,800 × *g*) to pellet proteins. The supernatant was transferred to a new tube and dried using a 96-well microplate evaporator (Apricot Designs Inc., Covina, CA) under N_2 at 50°C and reconstituted with 100 μl of 15% methanol containing 0.1% trifluoroacetic acid.

(*b*) Determination of drug concentration. The reconstituted samples (5-μl injection volume) were analyzed for drug concentration using a Waters Xevo TQ-S mass spectrometer (Foster City, CA) coupled with a Waters Acquity UPLC I-Class system. Compounds were separated on a

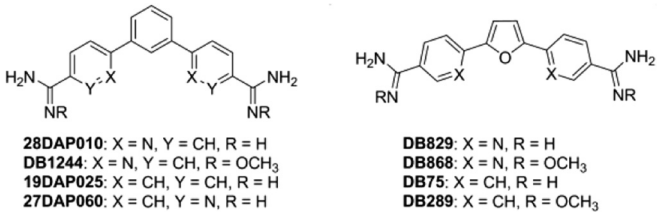

FIG 1 Chemical structures of 28DAP010, its prodrug DB1244, and its analogues.

Waters UPLC BEH C_{18} column (2.1 mm by 50 mm by 1.7 μm) equilibrated at 50°C. UPLC mobile phases consisted of water containing 0.1% formic acid (solution A) and methanol containing 0.1% formic acid (solution B). After a 0.15-min initial holding period at 10% solution B, mobile phase composition started with 10% solution B and was increased to 80% solution B over 2.2 min with a flow rate of 0.4 ml/min. Then the column was washed with 90% solution B for 0.5 min and was reequilibrated with 5% solution B for 1.1 min before injection of the next sample. The characteristic single reaction monitoring (SRM) transition for 28DAP010 and DB75-d8 were *m/z* 317.1→283.1 and 313.2→296.3, respectively, under positive electrospray ionization mode. The calibration curves for 28DAP010 ranged from 0.5 nM to 50 μM. The intraday coefficient of variation (CV) and accuracy were determined by measuring the same preparation of three standards three times on the same day. At concentrations of 5, 1,000, and 25,000 nM, the intraday CV and average accuracy of 28DAP010 quantification were 11.2% and 103%, 5.33% and 104%, and 0.70% and 106%, respectively.

(v) Pharmacokinetic analysis. The total area under the plasma concentration-time curve (AUC), terminal elimination half-life ($t_{1/2}$), maximum plasma drug concentration (C_{max}), time to reach C_{max} (T_{max}), clearance (CL), steady-state volume of distribution (V_{ss}), and mean residence time (MRT) were calculated using the trapezoidal rule-extrapolation method and noncompartmental analysis (WinNonlin version 5.0; Pharsight, Mountain View, CA).

RESULTS

Acute-stage *T. b. rhodesiense* mouse model. 28DAP010 and its two analogues 19DAP025 and 27DAP060 (Fig. 1) are highly active *in vitro* as well as *in vivo* against African trypanosomes (20). Within this study we analyzed the minimal curative dose in the stringent STIB900 acute-stage mouse model. All three compounds showed superior activity, curing all mice at 4 × 5 mg/kg i.p. or at single doses of 10 mg/kg i.p. (28DAP010 and 19DAP025) or 5 mg/kg i.p. (27DAP060) (20) (Table 2). Pentamidine cured only 1/4 mice at 4 × 5 mg/kg i.p. (23). *In vivo* efficacies of 28DAP010 and 19DAP025 were comparable. Cure rates of 3/4 or 2/4 mice were attained at a daily dose of 5 mg/kg i.p. or 1 mg/kg administered on 4 consecutive days. 27DAP060 was slightly more effective than 28DAP010 and 19DAP025. With the low dose of 4 × 0.25 mg/kg i.p., none of the 3 compounds were able to cure any of the mice, and the parasitemia relapses were detected already around 4 days after the last drug administration. 28DAP010 and its dipyridylfuran analogue DB829 showed similar efficacies in the STIB900 acute-stage mouse model (Table 2).

TABLE 3 *In vivo* antitrypanosomal activity of 28DAP010 in mice with GVR35 CNS infections

Dose regime (no. of doses × mg/kg[e])	No. of mice cured/no. infected				
	28DAP010	19DAP025	27DAP060	DB1244	DB829 or diminazene
5 × 25 i.p.	2/5, 5/6[a]	0/1[d]			4/5,[b] 6/6[a,b]
10 × 10 i.p.	0/5, 1/6[a]				
10 × 20 i.p.	5/5	0/1[d]	0/4		
5 × 100 p.o.				0/5	
1 × 40 i.p.					0/5[c]

[a] Cure obtained in a previous experiment.
[b] Result for DB829.
[c] Result for diminazene.
[d] Several mice died or were euthanized due to compound toxicity.
[e] No. of doses × mg/kg, one daily dose administered on consecutive days.

CNS *T. b. brucei* mouse model. The high efficacies in the acute-stage mouse model showed that the compounds merited further testing in the GVR35 CNS mouse model. 28DAP010 was the most potent compound among the three diamidines, curing all infected mice at 10 × 20 mg/kg i.p. (Table 3). The high CNS activity is exceptional, having been observed so far with only one other diamidine, DB829 (14).

The two analogues of 28DAP010—19DAP025 and 27DAP060—were both less effective and did not achieve any cures. Additionally, 19DAP025 was toxic and killed most of the mice at the dosages administered. 28DAP010 was also tested at 25 mg/kg for only 5 days and was almost as potent as DB829. This is only a slightly higher total dose than 10 mg/kg i.p. administered for 10 days but was clearly more effective (Table 3). 28DAP010 was well tolerated in NMRI mice at 5 × 25 mg/kg and 10 × 20 mg/kg i.p., without any overt toxicity observed.

The prodrug DB1244 is a methamidoxime derivative of 28DAP010 (analogous to DB868 being the methamidoxime derivative of DB829). It has been tested orally at 100 mg/kg administered on 5 consecutive days. At identical oral doses, DB1244 was

TABLE 2 *In vivo* antitrypanosomal activities of 28DAP010 and its analogues 19DAP010 and 27DAP060 (along with dipyridylfuran analogue DB829) in mice with acute-stage STIB900 *T. b. rhodesiense* infections[a]

Dose regime (no. of doses × mg/kg)	28DAP010 (*in vitro* IC_{50} [nM], 17 ± 4)		19DAP025 (*in vitro* IC_{50} [nM], 4 ± 1)		27DAP060 (*in vitro* IC_{50} [nM], 6 ± 1)		DB829 (*in vitro* IC_{50} [nM], 20 ± 4)	
	No. of mice cured/ no. infected	MRD	No. of mice cured/ no. infected	MRD	No. of mice cured/ no. infected	MRD	No. of mice cured/ no. infected	MRD
1 × 5 i.p.	3/4	17	2/4	17	4/4		2/4	53.5
1 × 10 i.p.	4/4		4/4		ND		4/4	
4 × 0.25 i.p.	0/4	12	0/4	9.25	0/4	13	0/4	14.75
4 × 1 i.p.	3/4	14	2/4	19	4/4		3/4	14
4 × 5 i.p.	4/4		4/4		4/4		4/4	

[a] DB1244, the methamidoxime prodrug of 28DAP010, cured 2/4 mice at 4 × 25 mg/kg p.o. (20). IC_{50}s are from references 20 and 23 and are expressed as means ± standard deviations. No. of doses × mg/kg, one daily dose administered on consecutive days; MRD, mean relapse day; ND, not determined.

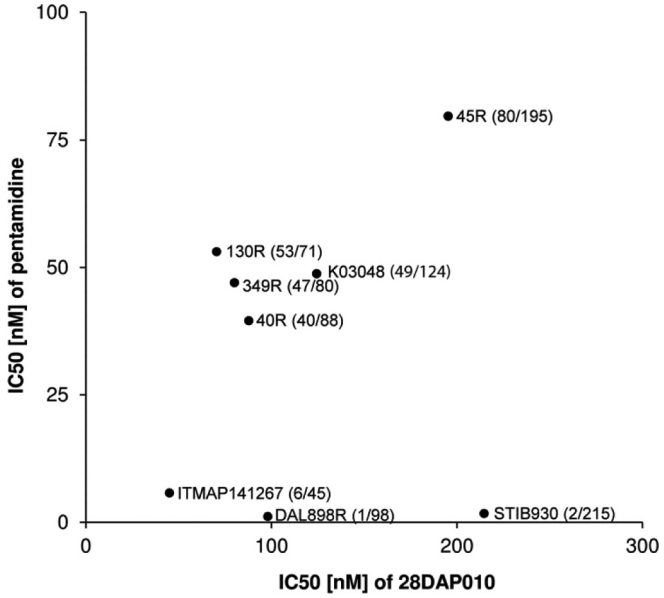

FIG 2 *In vitro* activities of pentamidine versus 28DAP010 against different *T. b. gambiense* strains. Symbols represent the average IC_{50} of at least three independent determinations. The first number in each set of parentheses represents the IC_{50} for pentamidine and the second number that for 28DAP010. No significant correlation was observed between pentamidine and 28DAP010 activities ($r^2 = 0.019$).

less potent in the CNS mouse model (no cures [Table 3]) than DB868 (5/5 mice cured) (14).

***In vitro* activity against different trypanosome strains.** We analyzed the *in vitro* activity of 28DAP010 against different trypanosome isolates in the alamarBlue viability assay. As most sleeping sickness patients suffer from *T. b. gambiense* infections, we tested 28DAP010 against several *T. b. gambiense* field isolates. The strains and culture conditions were identical to those used to determine the trypanocidal activity of DB829 (23), so the IC_{50}s of 28DAP010 and DB829 can therefore directly be compared. The *in vitro* IC_{50}s of 28DAP010 were higher for all tested *T. b. gambiense* isolates (IC_{50} = 45 to 215 nM [Fig. 2]) than for *T. b. rhodesiense* strain STIB900 (IC_{50} = 17 nM) and *T. b. brucei* strain BS221 (IC_{50} = 25 nM). Among the *T. b. gambiense* strains, there was no clear correlation between isolates from patients suffering from a relapse after melarsoprol treatment (strains whose name includes "R") and reduced potency of 28DAP010 (Fig. 2), whereas pentamidine appeared to be less active against strains that had been recently isolated (since 2003), which has also previously been shown (23). 28DAP010 was more active against the four "R" strains (130R, 349R, 40R, and DAL898R) than against the reference melarsoprol-sensitive strain STIB930. ITMAP141267 was the oldest isolate tested in this study (isolated in 1960 from the Democratic Republic of the Congo [DRC]), and it was the strain most sensitive to 28DAP010 and among those most sensitive to pentamidine (Fig. 2). However, no correlation in reduced trypanocidal activity among *T. b. gambiense* strains was observed between 28DAP010 and pentamidine (r^2 = 0.019) or with the isolates from melarsoprol-refractory patients.

We additionally studied the dependency of the P2 transporter for the uptake of 28DAP010 into trypanosomes using BS221Δ*AT1*, a P2 knockout strain (IC_{50} = 400 nM), and its corresponding wild type, BS221 (IC_{50} = 25 nM), by comparing the IC_{50}s determined in the alamarBlue assay. The resistance factor (RF) obtained with 28DAP010 on the P2 knockout strain (RF = 16) was comparable to the RF obtained by DB829 (14), suggesting that both compounds are taken up primarily by the P2 transporter.

***In vivo* mouse models with acute-stage infection with different *T. b. gambiense* isolates.** We assessed the efficacy of 28DAP010 in mice against four different *T. b. gambiense* isolates and compared the activity with that against *T. b. rhodesiense* STIB900 (Table 4). This was a crucial experiment since *in vitro*, 28DAP010 had been shown to be less active against the tested *T. b. gambiense* isolates than against *T. b. rhodesiense* strain STIB900 and *T. b. brucei* strain BS221. However, in *in vivo* experiments in mice, 28DAP010 was at least as efficacious for *T. b. gambiense* strains as for *T. b. rhodesiense* STIB900. 28DAP010 was curative at 1 × 20 mg/kg i.p. and at 4 × 5 mg/kg i.p. in STIB900-infected mice as well as in mice infected with either of the four *T. b. gambiense* strains (ITMAP141267, STIB930, 130R, and 45R), two of which (130R and 45R) were isolated from melarsoprol relapse patients. At a single dose of 5 mg/kg i.p., 28DAP010 cured 3/4 STIB900-infected mice, whereas all mice were cured of infection with the *T. b. gambiense* strains ITMAP141267 and STIB930 at the identical dose (Table 4). A group given a dose of 1 × 5 mg/kg i.p. was not included in the *in vivo* experiments with 130R and 45R, as the high efficacy with a 100% cure rate at a single dose of 20 mg/kg i.p. had not been expected prior to the experiment.

Time course of drug action *in vitro*. The time course of drug action of 28DAP010 *in vitro* versus the *T. b. rhodesiense* strain STIB900 and the two *T. b. gambiense* strains STIB930 and ITMAP141267 was recorded using isothermal microcalorimetry. Drug action was studied at different drug concentrations in 10-fold dilution steps ranging from 2 to 20,000 nM concentrations against the *T. b. rhodesiense* strain STIB900 or from 20 to 20,000 nM against the two *T. b. gambiense* strains. Four parameters were

TABLE 4 *In vitro* and *in vivo* antitrypanosomal activities of 28DAP010 against different *T. brucei* strains[a]

28DAP010 dose regime (no. of doses × mg/kg)	No. of mice cured/no. infected				
		T. b. gambiense			
	T. b. rhodesiense STIB900 (*in vitro* IC_{50} [nM], 17 ± 4)	ITMAP141267 (*in vitro* IC_{50} [nM], 45 ± 6)	STIB930 (*in vitro* IC_{50} [nM], 215 ± 56)	130R (*in vitro* IC_{50} [nM], 71 ± 33)	45R (*in vitro* IC_{50} [nM], 195 ± 50)
1 × 5 i.p.	3/4	4/4	3/3	ND	ND
1 × 20 i.p.	4/4	3/3	4/4	4/4	4/4
4 × 5 i.p.	4/4	4/4	4/4	4/4	4/4

[a] IC_{50}s are expressed as means ± standard deviations. No. of doses × mg/kg, one daily dose administered on consecutive days; ND, not determined.

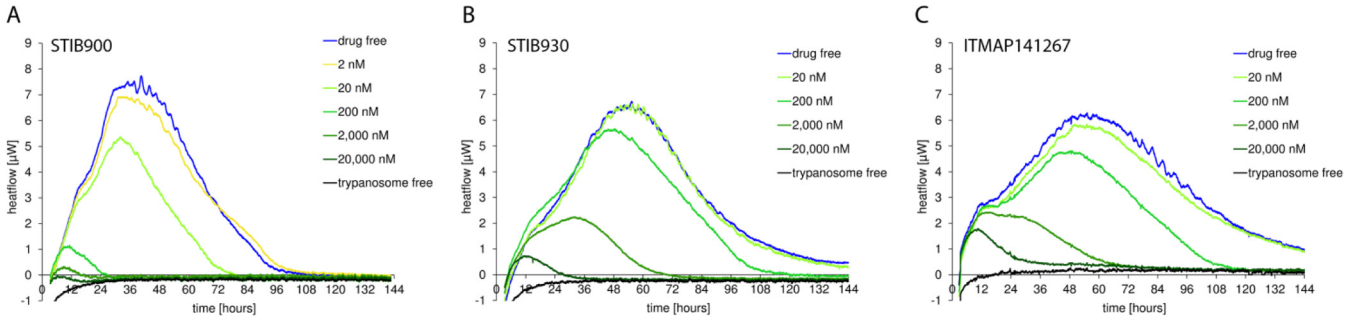

FIG 3 Microcalorimetry heat flow profiles of *T. b. rhodesiense* strain STIB900 (A) and *T. b. gambiense* strains STIB930 (B) and ITMAP141267 (C) in the presence of various concentrations of 28DAP010. Drug-free samples included parasites (5×10^4/ml inoculum) without drug treatment, and trypanosome-free experiment did not include any parasites or drug. Each curve represents the mean of three samples.

calculated from the curves for heat flow over time to describe the time course of drug action quantitatively: (i) the onset of drug action, (ii) the time to peak, (iii) the time to kill, and (iv) the growth rate (μ) and hence the level of growth inhibition ($1 - \mu_{drug}/\mu_{drug\ free}$) (23).

The time of drug action of 28DAP010 was concentration dependent (Fig. 3). The higher the concentration, the faster 28DAP010 acted and killed the parasites (in contrast to DB829, with which saturation was observed at ≥2,000 nM [23]). The onset of drug action on *T. b. rhodesiense* strain STIB900 ranged from <4 to 16 h, and the time to kill the parasite culture ranged from 24 to 92 h at concentrations of 20,000 to 20 nM (Table 5). At the highest tested drug concentration of 20,000 nM, drug action was so strong that not all parameters could be calculated. Also, the inhibition of the growth rate (μ) was dependent on the drug concentration, ranging from 7% at 2 nM up to >93% at the highest tested concentration of 20,000 nM.

Drug action of 28DAP010 *in vitro* was slower for *T. b. gambiense* strains ITMAP141267 and STIB930 (Fig. 3; Table 5) than for *T. b. rhodesiense* strain STIB900. This is consistent with the reduced activity (higher IC_{50}s) of 28DAP010 observed for *T. b. gambiense* in the alamarBlue assay. Growth of the two *T. b. gambiense* strains was also slightly slower in drug-free control cultures (μ = 0.018 to 0.024 h^{-1}, time to peak = 53 to 58 h, and time to overgrowth = 144 to 172 h) than that of *T. b. rhodesiense* strain STIB900 (μ = 0.029 h^{-1}, time to peak = 34 h, and time to overgrowth = 111 h) at identical trypanosome inocula of 5×10^4 trypanosomes/ml (Table 5). The onset of drug action for the two *T. b. gambiense* strains ranged from 5 to 30 h and the time to kill ranged from 46 to 126 h (2 to 5 days) at effective concentrations of 200 to 20,000 nM 28DAP010. Also, the inhibition of the growth rate (μ) was dependent on the drug concentration, ranging from 0.6 to 4% at 20 nM up to >82% at 20,000 nM for both *T. b. gambiense* strains (Table 5).

An inoculum effect is a phenomenon that has previously been observed with several diamidines. We studied the effect of two

TABLE 5 Drug action analysis of 28DAP010 by isothermal microcalorimetry

T. brucei strain[c]	Concn (nM)	Onset of action, mean (SD) (h)	Time to peak, mean (SD) (h)	Time to kill, mean (SD) (h)	Growth rate (μ), mean (SD) (h^{-1}/1,000)	Inhibition (%)[d]
STIB900	None (drug free)		34 (4)	111 (10)	29 (1)	
	2[a]	NM[e]	32 (8)	113 (7)	27 (1)	7
	20[a]	16 (3)	30 (7)	92 (5)	22 (2)	24
	200	7 (1)	10 (2)	49 (17)	7 (4)	76
	2,000	≤5[b]	10 (1)	32 (10)	3 (2)	>90
	20,000[b]	<4[b]	<9[b]	24 (7)	2[b]	>93
STIB930	None (drug free)		53 (2)	144 (8)	24 (2)	
	20[a]	NM	53 (2)	146 (5)	24 (1)	0.6
	200	30 (9)	50 (1)	126 (8)	23 (1)	4
	2,000	9 (2)	36 (3)	90 (8)	11 (2)	52
	20,000[b]	5[b]	13 (5)	46 (9)	4[b]	>82
ITMAP141267	None (drug free)		58 (4)	172 (11)	18 (3)	
	20[a]	NM	57 (4)	172 (7)	17 (3)	4
	200	21 (6)	47 (3)	124 (12)	16 (3)	11
	2,000	11 (4)	18 (6)	79 (7)	8 (1)	55
	20,000	6 (1)	10 (1)	47 (19)	3 (1)	85

[a] Inhibition is too small to recover parameters from every experiment performed accurately.
[b] Inhibition is too strong to recover parameters from every experiment performed accurately.
[c] Initial inoculum density was 5×10^4 trypanosomes/ml.
[d] Inhibition was determined as follows: $(1 - \mu_{drug}/\mu_{drug\ free}) \times 100$.
[e] NM, not measurable.

TABLE 6 Effects of inoculum and drug wash-out on drug action of 28DAP010 by isothermal microcalorimetry

T. brucei strain and inoculum	Concn (nM)	Onset of action, mean (SD) (h)	Time to peak, mean (SD) (h)	Time to kill, mean (SD) (h)	Growth rate (μ), mean (SD) (×1,000) (h^{-1})	Inhibition[e] (%)
STIB900						
5×10^4/ml	None (drug free)		38 (3)	118 (7)	27 (2)	
	20	14 (2)	33 (1)	93 (4)	22 (2)	19
	200	6 (1)	12 (1)	37 (3)	5 (1)	81
1×10^4/ml (low inoculum)	None (drug free)		50 (3)	125 (5)	27 (1)	
	20	12 (7)	29 (2)	59 (2)	4 (1)	85
	200[b]	9[b]	13[b]	25[b]	NM[a,b]	>98
5×10^4/ml, wash-out	None (drug free)		55 (4)	132 (11)	26 (2)	
	200	<30	45 (7)	82 (19)	6 (2)	77
STIB930						
5×10^4/ml	None (drug free)		50 (2)	148 (9)	24 (2)	
	200	26 (4)	50 (1)	121 (8)	23 (1)	6
	2,000	8 (2)	36 (3)	85 (7)	10 (2)	58
1×10^4/ml (low inoculum)	None (drug free)		68 (1)	160 (10)	24 (2)	
	200	27 (3)	52 (5)	100 (11)	12 (2)	51
	2,000[b]	<15[b]	31 (5)	60 (3)	2[b]	>93
5×10^4/ml, wash-out	None (drug free)		64 (5)	154 (11)	21 (1)	
	200[c]	<30	61 (2)	128 (9)	21 (1)	0
	2,000[d]	<30	60 (4)	130 (12)	15 (2)	28

[a] NM, not measurable.
[b] Inhibition is too strong to recover parameters from every experiment performed accurately.
[c] Only two independent experiments were performed (in triplicate).
[d] Only one independent experiment was performed (in triplicate).
[e] Inhibition was determined as follows: $(1 - \mu_{drug}/\mu_{drug\ free}) \times 100$.

different initial parasite densities (5×10^4/ml and 1×10^4/ml) on the sensitivity to 28DAP010 by isothermal microcalorimetry (see Fig. S1 in the supplemental material). With an inoculum of 5×10^4/ml, the growth rate of *T. b. rhodesiense* strain STIB900 was inhibited by 19% at 20 nM and 81% at 200 nM (Table 6). Considerably stronger inhibition was observed at the lower inoculum of 1×10^4/ml. The parasite culture was inhibited by 85% at 20 nM and >98% at 200 nM (Table 6; see also Fig. S1). In contrast, onset of drug action and time to peak of the heat flow curves remained similar with the different inocula (Table 6). The same phenomenon was observed in the experiments with *T. b. gambiense* strain STIB930. With an initial inoculum of 5×10^4/ml, parasite growth rate was inhibited by 6% at a drug concentration of 200 nM and by 58% at 2,000 nM. Stronger inhibitions were observed at the lower inoculum, with 51% at 200 nM and >93% at 2,000 nM (Table 6). The other two parameters, onset of action and time to peak of the heat flow curves, remained again similar at the different inocula. No clear inoculum effect was observed at 2 nM 28DAP010 (see Fig. S1).

Diamidines are normally taken up rapidly into trypanosomes, but parasite death is usually delayed. We tested whether continuous drug exposure is required for 28DAP010 to kill the trypanosomes or if an exposure of 24 h is sufficient to kill the parasites at a later time point. Inhibition of trypanosome cultures that were incubated for 24 h with 28DAP010 and then washed was monitored in drug-free culture medium by microcalorimetric analysis. The heat flow of preexposed trypanosome samples in drug-free culture medium was compared with that of parasites continuously exposed to the drug. The wash-out experiments were performed with two strains (STIB900 and STIB930).

The time to peak of the washed, drug-free samples was delayed by 14 to 17 h compared to the drug-free samples that were not washed (Table 6; see also Fig. S2 in the supplemental material). This delay was attributed to loss of some trypanosomes during the washing steps since both samples were set up and run simultaneously. The trypanosome culture was still alive, as seen by heat flow rate above baseline at the 24-h time point, and heat production did increase in the wash-out samples after any drug was removed. This indicates that the cells were still multiplying after the drug preexposure at a 200 or 2,000 nM concentration. However, the cultures in the drug-free medium did die after some time (see Fig. S2). The times to kill after drug wash-out were delayed compared to those with continuous drug exposure (82 versus 37 h) for *T. b. rhodesiense* strain STIB900 at 200 nM and for *T. b. gambiense* strain STIB930 (130 versus 85 h) at 2,000 nM (Table 6). However, the 24-h exposure was sufficient to kill STIB900 at 200 nM and STIB930 at 2,000 nM at the later time, which confirms that lethal concentrations were taken up within the first 24 h. With lower drug concentrations, a revival of the parasite culture after wash-out was observed in some cases: with STIB900 at 20 nM and with STIB930 at 200 nM (data not shown).

Pharmacokinetics and brain exposure of 28DAP010 after i.v. and i.p. administration in mice. The mean plasma concentration-time profiles of 28DAP010 were determined after a single i.v. dose of 7.5 μmol/kg (2.4 mg/kg) or a single i.p. dose of 65 μmol/kg (21 mg/kg) (Fig. 4). Both profiles exhibited at least a biphasic decline with an initial distribution phase and a terminal elimination phase. Pharmacokinetic outcomes were determined using noncompartmental analysis (Table 7). Following i.v. administration, the average plasma concentration of 28DAP010 reached 70.2 μM about 1 min after i.v. administration, but it quickly decreased, to below 1 μM by 2 h postdose and below 0.1 μM by 8 h postdose (Fig. 4A). The steady-state volume of distribution was 15 liters/kg, markedly greater than the physiologic fluid volume. The

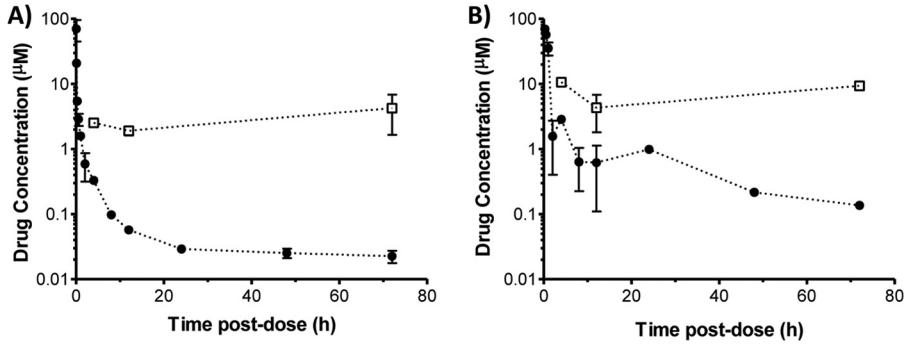

FIG 4 Plasma (filled circles) and brain (open squares) concentration-time profiles of 28DAP010 following intravenous (A) and intraperitoneal (B) administration to uninfected mice. The doses were 7.5 μmol/kg (or 2.4 mg/kg) for i.v. administration and 65 μmol/kg (or 21 mg/kg) for i.p. administration. Symbols and error bars represent means and standard errors of triplicate determinations, respectively.

average brain concentration of 28DAP010 was 4.2 μM at 72 h postdose, approximately 190-fold higher than the corresponding plasma concentration (Table 7). Following i.p. administration, 28DAP010 was rapidly absorbed into blood circulation, reaching a plasma C_{max} of 69.6 μM at 15 min postdose. The average plasma concentration of 28DAP010 decreased below 1 μM by 8 h postdose but remained above 0.1 μM for at least 72 h after injection (Fig. 4B). The average brain concentration of 28DAP010 was 9.3 μM at 72 h postdose, approximately 69-fold higher than the corresponding plasma concentration (Table 7).

The nonspecific binding of 28DAP010 to mouse plasma proteins and brain tissues was determined (Table 7). 28DAP010 showed moderate binding to mouse plasma ($f_{u,\ plasma}$ = 26.3%) but bound avidly to brain tissues ($f_{u,\ brain}$ = 0.69%).

TABLE 7 Pharmacokinetic parameters of 28DAP010 after i.v. and i.p. administration to uninfected mice

Compartment	Parameter[a]	Value for dosing route	
		i.v.	i.p.
Plasma	Dose, μmol/kg (mg/kg)	7.5 (2.4)	65 (21)
	$C_{5\ min}$, μmol/liter	20.8 ± 0.7[b]	NC[c]
	C_{max}, μmol/liter	70.2[d]	69.6
	T_{max}, h	NC	0.25
	$AUC_{0-\infty}$, μmol/liter · h	15	102
	$t_{1/2}$, h	68	26
	CL, liter/h/kg	0.50	NC
	V_{ss}, liters/kg	15	NC
	MRT, h	30	NC
	$f_{u,\ plasma}$, %	26.3 ± 2.2[b]	
Brain	C_{brain_72h}, μmol/liter	4.2 ± 4.5[b]	9.3 ± 0.5[b]
	AUC_{brain_0-72h}, μmol/liter · h	202	469
	B/P at 72 h	190	69
	$f_{u,\ brain}$, %	0.69 ± 0.07[b]	

[a] $C_{5\ min}$, plasma concentration at 5 min postdose; C_{max}, maximum plasma concentration; T_{max}, time to reach C_{max}; $AUC_{0-\infty}$, area under the plasma concentration-time curve from time zero to infinitity; $t_{1/2}$, terminal elimination half-life; CL, clearance; V_{ss}, steady-state volume of distribution; MRT, mean residence time; C_{brain_72h}, brain concentration at 72 h postdose; AUC_{brain_0-72h}, area under the brain concentration-time curve from time zero to 72 h postdose; B/P, brain-to-plasma concentration ratio; f_u, drug unbound fraction; $C_{5\ min}$, plasma concentration at 5 min postdose; B/P, brain-to-plasma concentration ratio.
[b] Mean ± standard deviation of triplicate determinations.
[c] NC, not calculated.
[d] Plasma concentration at 1 min postdose.

Time of drug action *in vivo*. The time of drug action of 28DAP010 *in vivo* was determined following a single i.p. dose of 20 mg/kg to mice infected with *T. b. rhodesiense* strain STIB900 or the *T. b. gambiense* strains ITMAP141267 and STIB930. The *in vivo* time to kill (parasite clearance time) of 28DAP010 was determined in the same experiment as the previously reported data for DB829 (23). Typically, diamidines are rather slow-acting compounds, especially DB829. Therefore, the first blood sample collected was 24 h after treatment. This time point is close to the parasite clearance time of 28DAP010, as in each group one mouse (STIB930 and ITMAP141267) or three of four mice (STIB900 infected) were already parasite free 24 h after drug administration.

The parasite clearance time was, on average, 26 h (24 to 32 h) when mice were infected with the *T. b. rhodesiense* strain STIB900 (Table 8). This is in the range of the *in vitro* time to kill at 2,000 to 20,000 nM concentrations (24 to 32 h [Table 5]). The time to kill for the *T. b. gambiense* strain ITMAP141267 was, on average, 42 h (24 to 56 h); that in STIB930-infected mice was 40 h (24 to 48 h) (Table 8), which is slightly faster than the *in vitro* time to kill at the two highest concentrations of 2,000 and 20,000 nM (Table 4).

DISCUSSION

Our studies of the diamidine 28DAP010 and its two analogues 27DAP060 and 19DAP025 showed that they are highly active against African trypanosomes *in vivo*. In the STIB900 acute-stage mouse model, the mice were cured by a single i.p. dose (Table 2) (20). However, among the three analogues, only 28DAP010 cured mice with second-stage infections in the GVR35 CNS mouse model (Table 3).

The availability of more efficacy data for a number of diami-

TABLE 8 *In vivo* time to kill (parasite clearance time) in infected mice after 28DAP010 treatment

T. brucei strain	Time to kill (h), mean (range)[a]
STIB900	26 (24–32)
ITMAP141267	42 (24–56)
STIB930	40 (24–48)

[a] 28DAP010 was given as a single dose at 20 mg/kg i.p. 3 days after infection. Values are means of four mice per group; ranges represents the time when the first and last mouse became aparasitemic.

dines makes it possible to consider some structure-activity relationships. 28DAP010 is chemically closely related to DB829 (Fig. 1). In the present study, 19DAP025 was less CNS potent and more toxic than its diaza analogue 28DAP010 (Table 3). Most of the infected mice died during or shortly after treatment with 19DAP025 at 5 × 25 mg/kg or 10 × 20 mg/kg i.p. A similar comparison can be made between furamidine and DB829 (14). 27DAP060, a regioisomer of 28DAP010, was highly active *in vivo* in the acute-stage mouse model (Table 2) but less CNS active than 28DAP010 (Table 3). This has been observed in previous experiments with aza analogues of furamidine (DB75) (24), in which only DB829 cured CNS-infected mice (14). The two pyridyl nitrogen atoms introduced in DB75 decreased the pK_a value of DB829 by only 1 unit, and it was still above physiological pH (36). The higher BBB penetration can therefore not be attributed to an effect on pK_a alone. The identical positions of the nitrogen atoms in the outer pyridine rings in both DB829 and 28DAP010 (Fig. 1) may play a crucial role in CNS potency and in the recognition of the molecules by a presumed transporter protein located at the BBB, which supports the penetration of 28DAP010 and DB829 into the brain. The CNS mouse model results for these two molecules confirm that certain diamidines do indeed have potential for curing not only first-stage but also second-stage HAT by the parenteral administration route.

There is still some interest in the use of prodrugs, particularly because of their potential for oral administration. Since the analogue DB868, the methamidoxime prodrug of DB829, cured mice showing CNS infection after oral administration (14), we analyzed the potency of DB1244, which is a methamidoxime prodrug of 28DAP010, in the GVR35 CNS mouse model at the same dosage. However, DB1244 was much less CNS active than DB868 (Table 3) (14), although its acute-stage mouse model activity was similar (Table 2) (14, 20). Further metabolism and pharmacokinetic studies of DB1244 are needed to explain the observed efficacy difference. When DB868 was tested by the oral route in vervet monkeys with second-stage infections, the therapeutic window was smaller for the prodrug DB868 than for its active diamidine DB829 (18). Measurement of the efficacy of 28DAP010 in the second-stage vervet monkey model will be needed for comparison with DB829.

Our greatest concern was to test the susceptibilities of different *T. b. gambiense* isolates to 28DAP010, as >98% of all HAT cases are due *T. b. gambiense* infections (2). Most of our strains were isolated from patients from the Democratic Republic of the Congo (DRC), the country harboring most HAT patients (1). We observed considerable reduction in the *in vitro* activity of 28DAP010 against the different *T. b. gambiense* strains compared to *T. b. rhodesiense* and *T. b. brucei* strains. This phenomenon has been observed previously with DB829 (against all tested *T. b. gambiense* isolates) and with pentamidine against recent isolates (K03048, 40R, 45R, 130R, and 349R) that were derived from patients within the last 10 years (23). However, our *in vivo* experiments with *T. b. gambiense* infections with four different isolates (ITMAP141267, STIB930, 130R, and 45R) were encouraging. 28DAP010 proved to be highly active against *T. b. gambiense* as well as *T. b. rhodesiense* isolates. The *T. b. gambiense*-infected mice were cured at doses comparable to, or even lower than, those used for mice infected with *T. b. rhodesiense* STIB900 (Table 4). The reduced *in vitro* activities of 28DAP010 and DB829 may be the result of factors that do not influence activity *in vivo*. They could be due to the slower growth of *T. b. gambiense* isolates or be the result of different culture conditions leading, for example, to a downregulation of a diamidine uptake transporter(s) (37) and thus to a reduced susceptibility of the *T. b. gambiense* isolates *in vitro* (23).

Cross-resistance between pentamidine and melamine-based arsenicals such as melarsoprol is a well-known phenomenon (38–40) involving the P2 transporter (41, 42). Therefore, we were concerned about a possible cross-resistance between 28DAP010 and these drugs or the possible development of more resistant trypanosome strains. Tests using a P2 knockout (KO) *T. brucei* strain indicated that the uptake of 28DAP010 is dependent on the P2 transporter. We observed a resistance factor ($IC_{50\ P2\text{-}KO}/IC_{50\ wild\ type}$) of 16, which was similar to that for DB829 and diminazene in the 72-h alamarBlue assay (14). Recently another transporter, aquaporin 2 (AQP2), was identified which is also involved in drug uptake and the development of resistance to pentamidine and melarsoprol (40, 43, 44). However, cross-resistance seems to be limited to the two diamidines pentamidine and 28DAP010, as the IC_{50}s of the two diamidines for different *T. b. gambiense* field isolates do not correlate ($r^2 = 0.019$) (Fig. 2). A similar effect was observed between pentamidine and diminazene (44). Analysis of *T. b. gambiense* field isolates with reduced susceptibility to pentamidine did reveal rearrangements of the *TbAQP2/TbAQP3* locus accompanied by *TbAQP2* gene loss (44). The mutant *T. b. gambiense* field isolates were less susceptible to pentamidine and melarsoprol but still susceptible to diminazene (44) and DB829 (23) and, as can be seen in Fig. 2, also to 28DAP010. Additionally, 28DAP010 was able to cure mice that were infected with recent *T. b. gambiense* isolates that were less susceptible to pentamidine *in vitro* (Table 4). Lack of AQP2 dependency for uptake of 28DAP010 and DB829 would explain why the recent *T. b. gambiense* isolates that were less susceptible to pentamidine were still sensitive to 28DAP010 and DB829.

An understanding of the pharmacokinetics and pharmacodynamics of drugs is necessary to develop effective treatment schedules. The time of drug action on trypanosomes can be determined *in vitro* using isothermal microcalorimetry (21). This method is based on the heat production of metabolically active parasites and thus allows studying the growth of cultures in the presence and absence of drugs (21, 23). It is simple to use and offers constant monitoring of a parasite population on a real-time basis (21).We analyzed the time of drug action of 28DAP010 at different concentrations on 3 different trypanosome strains. The time course of drug action was concentration dependent. No saturation could be observed with 28DAP010, whereas in experiments with DB829, saturation was found above 2,000 nM (23). This was probably due to saturation of the P2 transporter with DB829 (23, 37). It is possible that 28DAP010 is taken up by an additional high-capacity, low-affinity transporter at high drug concentrations, leading to a stronger drug action at concentrations above 2,000 nM.

We studied the inoculum effect of 28DAP010 by using identical drug concentrations but different initial parasite densities (inocula), 1×10^4/ml and 5×10^4/ml (see Fig. S1 in the supplemental material). We observed a strong inoculum effect on the growth rate (μ) and on the time to kill. However, the onset of drug action and the time to peak were less affected at the different trypanosome starting densities at identical drug concentrations, as can be observed at 20 and 200 nM concentrations with STIB900 or at 200 and 2,000 nM concentrations with STIB930 (Table 6). This indi-

cates that the drug action starts almost concurrently at the different starting densities using the same drug concentration. This phenomenon has been previously observed with DB829 and pentamidine in microcalorimetric studies (23). The major reason for the inoculum effect *in vitro* seems to be the concurrent onset of drug action, which appears at a much lower trypanosome density at the lower inoculum. Therefore, the inhibition of these compounds is more pronounced than for the drug-free control samples at the lower inoculum than at the higher inoculum.

The time taken to kill parasites is an important parameter to measure treatment efficacy. It has been shown that several diamidines (such as pentamidine, DB75, and DB829) are rapidly taken up by African trypanosomes; however, trypanosome death occurred much later (9, 23, 45, 46). We studied the drug action at effective concentrations (200 nM for STIB900 and 2,000 nM for STIB930) for an exposure time of 24 h, after which the drug was washed out (see Fig. S2 in the supplemental material). Growth was followed by isothermal microcalorimetry. After the drug had been washed out from the trypanosome culture, the parasites seemed to grow for at least one more day (see time to peak in Table 6). The trypanosomes were finally killed as a consequence of the 24-h drug exposure, but death occurred almost 2 days later than in continuously exposed trypanosomes (Table 6; see also Fig. S2). Microcalorimetric studies with multiple concentrations of 28DAP010 and multiple time points would be needed to examine this phenomenon in detail, but this was beyond the scope of this study. The performed wash-out experiments suggest that the high maximum drug concentration in plasma (C_{max}) after i.p. administration (Table 7) resulted in the high *in vivo* efficacy observed after a single i.p. dose with 28DAP010. The great *in vivo* efficacy in *T. b. rhodesiense*- and *T. b. gambiense*-infected mice (Tables 2 and 4) is not surprising considering the high C_{max} combined with the long half-life of 28DAP010.

28DAP010 showed a high brain-to-plasma concentration (B/P) ratio at 72 h postdose (Table 7), suggesting good CNS penetration. The high B/P ratio appears to be largely driven by the more extensive binding of 28DAP010 to brain tissue than to plasma ($f_{u,\ plasma}/f_{u,\ brain}$). However, it has been previously observed using fluorescence microscopy that DB75 did not distribute into brain parenchyma but sequestered within endothelial cells lining the BBB and blood-cerebrospinal fluid barrier. It is unknown whether 28DAP010 was also sequestered within the endothelial cells or distributed more extensively into brain parenchyma. Nonetheless, the observed high B/P ratio and efficacy in the CNS *T. b. brucei* mouse model support 28DAP010 as a CNS-active trypanocide.

The speed at which drugs act is of varying clinical importance. Fast elimination of the parasite is not as vital for HAT patients as it is for patients infected with some other parasites, like malaria parasites, which cause much more rapid death. However, fast-acting drugs are of advantage to minimize the risk of resistant parasite selection in the patient and to reduce the hospitalization time. *In vitro* as well as *in vivo*, 28DAP010 was faster acting than DB829. However, a short exposure to 28DAP010 or to DB829 (23) was sufficient to kill the trypanosomes in a delayed manner (Table 6). High drug levels therefore do not need to be maintained over the entire parasite clearance time *in vivo*.

More problematic than a relatively slow speed of action are undesirable side effects such as hepatotoxicity or nephrotoxicity. Such effects have been observed for pentamidine (47) and DB289 (pafuramidine) (15, 16, 48), and the nephrotoxicity of pafuramidine actually led to the termination of the clinical studies (16). It is encouraging that studies with rats and mice indicate that nephrotoxicity is not clearly class related (49). DB829 (resulting from DB868 administration) accumulated less in liver and kidneys than did DB75 (after pafuramidine administration) (16). The toxicity profile of 28DAP010 may also differ from that observed for pafuramidine.

Second-stage efficacy of DB829 has been demonstrated in the mouse (14) and monkey (18) models. In the present study, 28DAP010 revealed similar efficacies in mouse models. Both molecules are able to cure both disease stages and infections with both studied subspecies, *T. b. gambiense* and *T. b. rhodesiense*, at low and tolerated doses. Extensive toxicity studies of 28DAP010 and DB829 side by side are still needed. Drug tolerability will be an important criterion for choosing the better of these two diamidines for further drug development.

There is a continuing discussion about the relative advantages and disadvantages of prodrugs and intrinsically active compounds. The use of an orally active prodrug to cure second-stage HAT could be helpful in resource-poor settings. However, parenteral administration also has advantages. The use of an active diamidine will simplify the pharmacokinetic and toxicity analyses that will be needed if the drug is to be used, and treatment with one of the backup compounds, 28DAP010 or DB829, could be short and simple. Treatment duration of 5 days or less for second stage could well be feasible and could be tested for further development for HAT on the basis of the favorable pharmacokinetics after parenteral administration.

A sustained drug development pipeline will increase the chance of getting a new and improved treatment into the market (19). This will help to control, and eventually to eliminate, the disease (50, 51). With 28DAP010, we have found a new promising backup diamidine as a preclinical candidate for the treatment of first- and second-stage African sleeping sickness.

ACKNOWLEDGMENTS

We thank Pati Pyana and Anne Clarisse Lekane Likeufack for collecting *T. b. gambiense* strains from patients in the Democratic Republic of the Congo, Guy Riccio and Christiane Braghiroli for carrying out experiments for *in vivo* efficacy and time to kill in mice, and Kirsten Gillingwater for help with the time-to-kill experiments in mice. We also thank Jennifer Jenkins for critical reading and input to the manuscript.

This work was supported by the Bill and Melinda Gates Foundation through the Consortium for Parasitic Drug Development (CPDD) and by the Swiss Tropical and Public Health Institute.

REFERENCES

1. **Simarro PP, Cecchi G, Franco JR, Paone M, Fèvre EM, Diarra A, Postigo JAR, Mattioli RC, Jannin JG.** 2011. Risk for human African trypanosomiasis, Central Africa, 2000–2009. Emerg. Infect. Dis. **17:**2322–2324. http://dx.doi.org/10.3201/eid1712.110921.
2. **WHO.** 2014. Trypanosomiasis, human African (sleeping sickness). Fact sheet no. 259. WHO, Geneva, Switzerland.
3. **Brun R, Don R, Jacobs RT, Wang MZ, Barrett MP.** 2011. Development of novel drugs for human African trypanosomiasis. Future Microbiol. **6:**677–691. http://dx.doi.org/10.2217/fmb.11.44.
4. **Blum J, Schmid C, Burri C.** 2006. Clinical aspects of 2541 patients with second stage human African trypanosomiasis. Acta Trop. **97:**55–64. http://dx.doi.org/10.1016/j.actatropica.2005.08.001.
5. **Brun R, Blum J, Chappuis F, Burri C.** 2010. Human African trypanosomiasis. Lancet **375:**148–159. http://dx.doi.org/10.1016/S0140-6736(09)60829-1.

6. **Soeiro MNC, de Castro SL, de Souza EM, Batista DGJ, Silva CF, Boykin DW.** 2008. Diamidine activity against trypanosomes: the state of the art. Curr. Mol. Pharmacol. **1:**151–161. http://dx.doi.org/10.2174/1874467210801020151.
7. **Sands M, Kron MA, Brown RB.** 1985. Pentamidine: a review. Rev. Infect. Dis. **7:**625–634. http://dx.doi.org/10.1093/clinids/7.5.625.
8. **Peregrine AS, Mamman M.** 1993. Pharmacology of diminazene: a review. Acta Trop. **54:**185–203. http://dx.doi.org/10.1016/0001-706X(93)90092-P.
9. **Werbovetz K.** 2006. Diamidines as antitrypanosomal, antileishmanial and antimalarial agents. Curr. Opin. Investig. Drugs **7:**147–157.
10. **Wang MZ, Saulter JY, Usuki E, Cheung Y-L, Hall M, Bridges AS, Loewen G, Parkinson OT, Stephens CE, Allen JL, Zeldin DC, Boykin DW, Tidwell RR, Parkinson A, Paine MF, Hall JE.** 2006. CYP4F enzymes are the major enzymes in human liver microsomes that catalyze the O-demethylation of the antiparasitic prodrug DB289 [2,5-bis(4-amidinophenyl)furan-bis-O-methylamidoxime]. Drug Metab. Dispos. **34:**1985–1994. http://dx.doi.org/10.1124/dmd.106.010587.
11. **Wang MZ, Wu JQ, Bridges AS, Zeldin DC, Kornbluth S, Tidwell RR, Hall JE, Paine MF.** 2007. Human enteric microsomal CYP4F enzymes O-demethylate the antiparasitic prodrug pafuramidine. Drug Metab. Dispos. **35:**2067–2075. http://dx.doi.org/10.1124/dmd.107.016428.
12. **Saulter JY, Kurian JR, Trepanier LA, Tidwell RR, Bridges AS, Boykin DW, Stephens CE, Anbazhagan M, Hall JE.** 2005. Unusual dehydroxylation of antimicrobial amidoxime prodrugs by cytochrome b5 and NADH cytochrome b5 reductase. Drug Metab. Dispos. **33:**1886–1893. http://dx.doi.org/10.1124/dmd.105.005017.
13. **Midgley I, Fitzpatrick K, Taylor LM, Houchen TL, Henderson SJ, Wright SJ, Cybulski ZR, John BA, McBurney A, Boykin DW, Trendler KL.** 2007. Pharmacokinetics and metabolism of the prodrug DB289 (2,5-bis[4-(n-methoxyamidino)phenyl]furan monomaleate) in rat and monkey and its conversion to the antiprotozoal/antifungal drug DB75 (2,5-bis(4-guanylphenyl)furan dihydrochloride). Drug Metab. Dispos. **35:**955–967. http://dx.doi.org/10.1124/dmd.106.013391.
14. **Wenzler T, Boykin DW, Ismail MA, Hall JE, Tidwell RR, Brun R.** 2009. New treatment option for second-stage African sleeping sickness: in vitro and in vivo efficacy of aza analogs of DB289. Antimicrob. Agents Chemother. **53:**4185–4192. http://dx.doi.org/10.1128/AAC.00225-09.
15. **Burri C.** 2010. Chemotherapy against human African trypanosomiasis: is there a road to success? Parasitology **137:**1987–1994. http://dx.doi.org/10.1017/S0031182010001137.
16. **Paine MF, Wang MZ, Generaux CN, Boykin DW, Wilson WD, De Koning HP, Olson CA, Pohlig G, Burri C, Brun R, Murilla GA, Thuita JK, Barrett MP, Tidwell RR.** 2010. Diamidines for human African trypanosomiasis. Curr. Opin. Investig. Drugs **11:**876–883.
17. **Hu L, Patel A, Bondada L, Yang S, Wang MZ, Munde M, Wilson WD, Wenzler T, Brun R, Boykin DW.** 2013. Synthesis and antiprotozoal activity of dicationic 2,6-diphenylpyrazines and aza-analogues. Bioorg. Med. Chem. **21:**6732–6741. http://dx.doi.org/10.1016/j.bmc.2013.08.006.
18. **Thuita JK.** 2013. Biological and pharmacological investigations of novel diamidines in animal models of human African trypanosomiasis. Ph.D. thesis. University of Basel, Basel, Switzerland.
19. **Mäser P, Wittlin S, Rottmann M, Wenzler T, Kaiser M, Brun R.** 2012. Antiparasitic agents: new drugs on the horizon. Curr. Opin. Pharmacol. **12:**562–566. http://dx.doi.org/10.1016/j.coph.2012.05.001.
20. **Patrick DA, Ismail MA, Arafa RK, Wenzler T, Zhu X, Pandharkar T, Jones SK, Werbovetz KA, Brun R, Boykin DW, Tidwell RR.** 2013. Synthesis and antiprotozoal activity of dicationic m-terphenyl and 1,3-dipyridylbenzene derivatives. J. Med. Chem. **56:**5473–5494. http://dx.doi.org/10.1021/jm400508e.
21. **Wenzler T, Steinhuber A, Wittlin S, Scheurer C, Brun R, Trampuz A.** 2012. Isothermal microcalorimetry, a new tool to monitor drug action against *Trypanosoma brucei* and *Plasmodium falciparum*. PLoS Negl. Trop. Dis. **6:**e1668. http://dx.doi.org/10.1371/journal.pntd.0001668.
22. **Wilson WD, Tanious FA, Mathis A, Tevis D, Hall JE, Boykin DW.** 2008. Antiparasitic compounds that target DNA. Biochimie **90:**999–1014. http://dx.doi.org/10.1016/j.biochi.2008.02.017.
23. **Wenzler T, Yang S, Braissant O, Boykin DW, Brun R, Wang MZ.** 2013. Pharmacokinetics, Trypanosoma brucei gambiense efficacy, and time of drug action of DB829, a preclinical candidate for treatment of second-stage human African trypanosomiasis. Antimicrob. Agents Chemother. **57:**5330–5343. http://dx.doi.org/10.1128/AAC.00398-13.
24. **Ismail MA, Brun R, Easterbrook JD, Tanious FA, Wilson WD, Boykin DW.** 2003. Synthesis and antiprotozoal activity of aza-analogues of furamidine. J. Med. Chem. **46:**4761–4769. http://dx.doi.org/10.1021/jm0302602.
25. **Stephens CE, Patrick DA, Chen H, Tidwell RR, Boykin DW.** 2001. Synthesis of deuterium-labelled 2,5-bis(4-amidinophenyl)furan, 2,5-bis[4-(methoxyamidino)phenyl]furan, and 2,7-diamidinocarbazole. J. Labelled Comp. Radiopharm. **44:**197–208. http://dx.doi.org/10.1002/jlcr.444.
26. **Räz B, Iten M, Grether-Bühler Y, Kaminsky R, Brun R.** 1997. The Alamar Blue assay to determine drug sensitivity of African trypanosomes (*T. b. rhodesiense* and *T. b. gambiense*) in vitro. Acta Trop. **68:**139–147. http://dx.doi.org/10.1016/S0001-706X(97)00079-X.
27. **Development Core Team R.** 2013. R: a language and environment for statistical computing. R Foundation for Statistical Computing, Vienna, Austria.
28. **Chambers JM, Hastie TJ.** 1992. Statistical models in S. Chapman & Hall/CRC, Boca Raton, FL.
29. **Hastie TJ, Tibshirani RJ.** 1990. Generalized additive models. Chapman & Hall, New York, NY.
30. **Legendre P, Legendre LFJ.** 1998. Numerical ecology. Elsevier, Amsterdam, Netherlands.
31. **Braissant O, Bonkat G, Wirz D, Bachmann A.** 2013. Microbial growth and isothermal microcalorimetry: growth models and their application to microcalorimetric data. Thermochim. Acta **555:**64–71. http://dx.doi.org/10.1016/j.tca.2012.12.005.
32. **Wang Y, Utzinger J, Saric J, Li JV, Burckhardt J, Dirnhofer S, Nicholson JK, Singer BH, Brun R, Holmes E.** 2008. Global metabolic responses of mice to *Trypanosoma brucei brucei* infection. Proc. Natl. Acad. Sci. U. S. A. **105:**6127–6132. http://dx.doi.org/10.1073/pnas.0801777105.
33. **Jennings FW, McNeil PE, Ndung'u JM, Murray M.** 1989. Trypanosomiasis and encephalitis: possible aetiology and treatment. Trans. R. Soc. Trop. Med. Hyg. **83:**518–519. http://dx.doi.org/10.1016/0035-9203(89)90272-1.
34. **Yan GZ, Brouwer KLR, Pollack GM, Wang MZ, Tidwell RR, Hall JE, Paine MF.** 2011. Mechanisms underlying differences in systemic exposure of structurally similar active metabolites: comparison of two preclinical hepatic models. J. Pharmacol. Exp. Ther. **337:**503–512. http://dx.doi.org/10.1124/jpet.110.177220.
35. **Kalvass JC, Maurer TS.** 2002. Influence of nonspecific brain and plasma binding on CNS exposure: implications for rational drug discovery. Biopharm. Drug Dispos. **23:**327–338. http://dx.doi.org/10.1002/bdd.325.
36. **Yang S, Wenzler T, Miller PN, Wu H, Boykin DW, Brun R, Wang MZ.** 5 May 2014. Mechanisms underlying the differential efficacy of cationic diamidines against first and second stage human African trypanosomiasis: a pharmacokinetic comparison. Antimicrob. Agents Chemother. http://dx.doi.org/10.1128/AAC.02605-14.
37. **Ward CP, Wong PE, Burchmore RJ, de Koning HP, Barrett MP.** 2011. Trypanocidal furamidine analogues: influence of pyridine nitrogens on trypanocidal activity, transport kinetics, and resistance patterns. Antimicrob. Agents Chemother. **55:**2352–2361. http://dx.doi.org/10.1128/AAC.01551-10.
38. **Williamson J, Rollo IM.** 1959. Drug resistance in trypanosomes; cross-resistance analyses. Br. J. Pharmacol. Chemother. **14:**423–430. http://dx.doi.org/10.1111/j.1476-5381.1959.tb00946.x.
39. **Bernhard SC, Nerima B, Mäser P, Brun R.** 2007. Melarsoprol- and pentamidine-resistant *Trypanosoma brucei rhodesiense* populations and their cross-resistance. Int. J. Parasitol. **37:**1443–1448. http://dx.doi.org/10.1016/j.ijpara.2007.05.007.
40. **Baker N, de Koning HP, Mäser P, Horn D.** 2013. Drug resistance in African trypanosomiasis: the melarsoprol and pentamidine story. Trends Parasitol. **29:**110–118. http://dx.doi.org/10.1016/j.pt.2012.12.005.
41. **Mäser P, Sütterlin C, Kralli A, Kaminsky R.** 1999. A nucleoside transporter from *Trypanosoma brucei* involved in drug resistance. Science **285:**242–244. http://dx.doi.org/10.1126/science.285.5425.242.
42. **Matovu E, Stewart ML, Geiser F, Brun R, Mäser P, Wallace LJM, Burchmore RJ, Enyaru JCK, Barrett MP, Kaminsky R, Seebeck T, de Koning HP.** 2003. Mechanisms of arsenical and diamidine uptake and resistance in *Trypanosoma brucei*. Eukaryot. Cell **2:**1003–1008. http://dx.doi.org/10.1128/EC.2.5.1003-1008.2003.
43. **Baker N, Glover L, Munday JC, Aguinaga Andrés D, Barrett MP, de Koning HP, Horn D.** 2012. Aquaglyceroporin 2 controls susceptibility to melarsoprol and pentamidine in African trypanosomes. Proc. Natl. Acad. Sci. U. S. A. **109:**10996–11001. http://dx.doi.org/10.1073/pnas.1202885109.

44. **Graf FE, Ludin P, Wenzler T, Kaiser M, Brun R, Pyana PP, Büscher P, de Koning HP, Horn D, Mäser P.** 2013. Aquaporin 2 mutations in *Trypanosoma brucei gambiense* field isolates correlate with decreased susceptibility to pentamidine and melarsoprol. PLoS Negl. Trop. Dis. **7:**e2475. http://dx.doi.org/10.1371/journal.pntd.0002475.
45. **Mathis AM, Bridges AS, Ismail MA, Kumar A, Francesconi I, Anbazhagan M, Hu Q, Tanious FA, Wenzler T, Saulter J, Wilson WD, Brun R, Boykin DW, Tidwell RR, Hall JE.** 2007. Diphenyl furans and aza analogs: effects of structural modification on in vitro activity, DNA binding, and accumulation and distribution in trypanosomes. Antimicrob. Agents Chemother. **51:**2801–2810. http://dx.doi.org/10.1128/AAC.00005-07.
46. **Berger BJ, Carter NS, Fairlamb AH.** 1995. Characterisation of pentamidine-resistant *Trypanosoma brucei brucei*. Mol. Biochem. Parasitol. **69:**289–298. http://dx.doi.org/10.1016/0166-6851(94)00215-9.
47. **Turner PR, Denny WA.** 1996. The mutagenic properties of DNA minor-groove binding ligands. Mutat. Res. **355:**141–169. http://dx.doi.org/10.1016/0027-5107(96)00027-9.
48. **Harrill AH, Desmet KD, Wolf KK, Bridges AS, Eaddy JS, Kurtz CL, Hall JE, Paine MF, Tidwell RR, Watkins PB.** 2012. A mouse diversity panel approach reveals the potential for clinical kidney injury due to DB289 not predicted by classical rodent models. Toxicol. Sci. Off. J. Soc. Toxicol. **130:**416–426. http://dx.doi.org/10.1093/toxsci/kfs238.
49. **Wolf KK, DeSmet K, Bridges A, Tidwell R, Paine MF, Hall JE, Watkins PB.** 2012. Two structurally similar anti-parasitic prodrugs differ markedly in toxicity profilesabstr ID2928. Soc. Toxicol. Annu. Meet. Abstr. Suppl.
50. **Simarro PP, Diarra A, Ruiz Postigo JA, Franco JR, Jannin JG.** 2011. The Human African Trypanosomiasis Control and Surveillance Programme of the World Health Organization 2000–2009: the way forward. PLoS Negl. Trop. Dis. **5:**e1007. http://dx.doi.org/10.1371/journal.pntd.0001007.
51. **Maurice J.** 2013. New WHO plan targets the demise of sleeping sickness. Lancet **381:**13–14. http://dx.doi.org/10.1016/S0140-6736(13)60006-9.
52. **Brun R, Schumacher R, Schmid C, Kunz C, Burri C.** 2001. The phenomenon of treatment failures in human African trypanosomiasis. Trop. Med. Int. Health **6:**906–914. http://dx.doi.org/10.1046/j.1365-3156.2001.00775.x.
53. **Jennings FW, Gray GD.** 1983. Relapsed parasitaemia following chemotherapy of chronic *T. brucei* infections in mice and its relation to cerebral trypanosomes. Contrib. Microbiol. Immunol. **7:**147–154.
54. **Felgner P, Brinkmann U, Zillmann U, Mehlitz D, Abu-Ishira S.** 1981. Epidemiological studies on the animal reservoir of *gambiense* sleeping sickness. Part II. Parasitological and immunodiagnostic examination of the human population. Tropenmed. Parasitol. **32:**134–140.
55. **Likeufack ACL, Brun R, Fomena A, Truc P.** 2006. Comparison of the in vitro drug sensitivity of *Trypanosoma brucei gambiense* strains from West and Central Africa isolated in the periods 1960–1995 and 1999–2004. Acta Trop. **100:**11–16. http://dx.doi.org/10.1016/j.actatropica.2006.09.003.
56. **Pyana PP, Ngay Lukusa I, Mumba Ngoyi D, Van Reet N, Kaiser M, Karhemere Bin Shamamba S, Büscher P.** 2011. Isolation of *Trypanosoma brucei gambiense* from cured and relapsed sleeping sickness patients and adaptation to laboratory mice. PLoS Negl. Trop. Dis. **5:**e1025. http://dx.doi.org/10.1371/journal.pntd.0001025.
57. **Maina N, Maina KJ, Mäser P, Brun R.** 2007. Genotypic and phenotypic characterization of *Trypanosoma brucei gambiense* isolates from Ibba, South Sudan, an area of high melarsoprol treatment failure rate. Acta Trop. **104:**84–90. http://dx.doi.org/10.1016/j.actatropica.2007.07.007.